

## NASA Technical Memorandum 100510

# STRUCTURAL ANALYSIS OF THE SPACE SHUTTLE SOLID ROCKET BOOSTER/EXTERNAL TANK ATTACH RING

(NASA-TM-100510) STRUCTURAL ANALYSIS OF THE SPACE SHUTTLE SOLID ROCKET BOOSTER/EXTERNAL TANK ATTACH RING (NASA) 32 P CSCI 22B

N88-18618

Unclas  
G3/18 0129395

John T. Dorsey

January 1988



National Aeronautics and  
Space Administration

Langley Research Center  
Hampton, Virginia 23665-5225

# STRUCTURAL ANALYSIS OF THE SPACE SHUTTLE SOLID ROCKET BOOSTER/EXTERNAL TANK ATTACH RING

John T. Dorsey  
NASA Langley Research Center  
Hampton, VA 23665

## INTRODUCTION

Following the Challenger accident (flight 51-L), the flight performance of many of the Shuttle system components, including the SRB/ET attach ring, were reviewed. Two problems were identified for the existing attach ring design; 1) negative margins of safety were calculated to occur at four locations, and 2) failed web-to-cap and web-to-tang fasteners had been recorded for a substantial number of SRBs recovered from flight. Tests and analyses confirmed that negative margins of safety existed in the ET attach ring assembly when the SRB motor case was pressurized (that is, under flight conditions), leading to the requirement that the ET attach ring be redesigned. Consequently, NASA Langley Research Center entered into a joint activity with NASA Marshall Space Flight Center to redesign the 270-degree partial ring and eliminate all negative margins of safety (see reference 1). Previously however, United Space Boosters, Inc. (Marshall Space Flight Center's ET attach ring prime contractor) chose to proceed with a full 360-degree redesign for the ET attach ring. A redesigned partial ring is desirable however, because of the substantial weight savings and reduced aerodynamic drag relative to the full 360-degree ring design.

The analyses discussed in this report were performed to aid the redesign effort for the 270-degree ring at Langley and had several objectives. The first objective was to provide ring stresses away from the ring ends (most of the design changes were at the ring ends) as input for more detailed ring redesign analyses. The second objective was to understand the stress distribution in the attach ring and SRB motor case during SRB pressurization and also, to assess the relative importance of the rocket motor axial and circumferential loading components on the stresses. The third objective was to determine the effect of geometric nonlinearities on ring stresses. The fourth and final objective was to determine the effect of the field joint, located 20 inches above the attach ring, on attach ring stresses.

All of the analyses were performed using a finite element model of the 270-degree partial ring design as flown on flight 51-L and previous flights. Details of the the finite element model and modeling assumptions, the boundary conditions, and the applied loadings are

described in this report. Analysis results from both linear and geometric nonlinear analyses, as well as conclusions are also discussed.

### EXTERNAL TANK ATTACH RING DESCRIPTION

The major components of the Space Shuttle system, as shown in figure 1a, are; the Orbiter, the External Tank (ET), and the two Solid Rocket Boosters (SRBs). The SRBs are attached to the aft end of the ET through a partial ring structure. The center of this SRB/ET attach ring is located at station 1511, which is 1511 inches from the top of the booster. This station is approximately 20 inches below the aft attachment segment field joint.

The purpose of the ET attach ring is to transfer lateral loads between the SRB and the ET. The loads are transferred through three struts which connect the SRB/ET attach ring assembly to the ET. The ET attach ring assembly consists of two tapered webs, three H-fittings for attaching the ET struts, cover plates, intercostals, brackets, and other subsystems. The ET attach ring assembly extends approximately 270-degrees circumferentially around the SRM segment (see figure 1b).

The webs of the ET attach ring are bolted at 2-degree circumferential increments to two integrally machined tangs on a SRB motor case segment, as shown in figure 2. The SRB motor case is thickened locally to .58 inches (from a nominal thickness of .479 inches) in the vicinity of the ring, and the two integrally machined tangs protrude 1.654 inches from the motor case outer surface. The two webs are constructed of 4130 steel, are .25 inches thick, and are, nominally, approximately 7 inches wide, tapering to about 2 inches wide at the ends. The distance between the two webs is 12 inches. Caps machined out of 4340 steel are attached to the tops of each web using 1/4 inch Hi-lok fasteners, and a cover plate is attached to the tops of the caps to complete the assembly.

### FINITE ELEMENT ANALYSIS MODEL

The SRB/ET attach ring which was modeled is the design which flew on mission 51-L. Although most of the analysis effort concentrates on obtaining stresses in the ET attach ring, information about the interaction between the attach ring and the SRB motor case wall is also desired, and thus, the finite element model also includes a length of the motor case. The finite element model captures all of the global behavior of the ET attach ring assembly but is considered simplified because the model does not contain structural details such as H-fittings, splice plates, intercostals, or tang-to-web and web-to-cap bolts. The fidelity of the model was chosen to reduce computer run times, especially for the

nonlinear analyses. One result of not modeling the individual tang-to-web and web-to-cap bolts is that the ET attach ring behaves as if it is welded to the tang, and as if all of the ring components are welded together.

### Model Description

The complete finite element model is shown in figure 3a and a view looking down the Z axis, which shows the web planform, is shown in figure 3b. The Engineering Analysis Language finite element program (reference 2) was used to model the ET attach ring and perform all linear and nonlinear analyses. The nominal inner radius for the SRB motor case wall is 72.54 inches and the nominal wall thickness is .479 inches, which gives an R/t value of 151 for the motor case (that is, thin shell theory applies). For a steel cylindrical shell with these physical properties, calculations derived from reference 3 give a characteristic shell length of approximately 18 inches. Thus, the finite element model must extend at least 18 inches beyond any change in shell stiffness for the moments caused by the stiffness change to become negligible. Two locations where changes in stiffness occur, are at the SRB motor case wall where the ET attach ring attaches to the case, and where the case wall changes thickness from .58 inches to .479 inches.

A cross section of the finite element model taken through the uniform portion of the web (section A-A on figure 3b) is shown in figure 4. In order to limit the size of the finite element model, a symmetry plane is assumed to exist half way between the two ET attach ring webs ( $Z=0$ . inches location), as shown at the top of the figure. The finite element model is comprised of five components; the SRB motor case wall (shell), the tang, the web, the cap, and the cover plate. All of the components in the model are assumed to be made of steel and have a Young's modulus of 30.0 million psi. The model has a total of 13,000 degrees of freedom and 2517 elements.

The SRB motor case wall is represented by 1528 plate elements having a thickness of 0.58 inches in the vicinity of the attach ring. Between  $Z=-10.685$  inches and  $Z=-12.435$  inches, the case wall thickness is reduced to 0.5295 inches to represent the section of tapered case wall. Below  $Z=-12.435$  inches, the shell is the nominal thickness of 0.479 inches. The shell is modeled 22 inches beyond this location to achieve a uniform membrane stress state, leading to the total model length of 34.435 inches shown in figure 4.

In the finite element model, the center of the web and the center of the tang are both assumed to be located at  $Z=-5.985$  inches as shown. The tang is integrally machined from the SRB motor case wall and

extends the full 360-degrees circumferentially around the motor case. The tang is modeled with 191 beam elements having a solid rectangular cross-section. Rigid offsets on the beam ends are used to locate the tang's geometric center at the proper radius from the nodes representing the case wall centerline.

The web is modeled with 520 plate elements, all having a thickness of .25 inches. The number of plate elements through the width is four for most of the web except at the ends, where web tapering reduces the number of elements through the width to two. Rigid offsets are used to locate the base of the web at the proper radius from the line of joints representing the motor case wall (see figure 4).

The cap, which extends all the way to the end of the web on one end and near the end on the other, is represented by 137 beam elements with a solid rectangular cross-section. Rigid offsets are used to place the geometric center of the cap at the proper location from the top of the web.

Physically, the cover plate is slotted circumferentially, so that when it is bolted to the top of the cap, it will not add any circumferential stiffness to the attach ring. The cover plate does provide stiffness in the booster longitudinal direction however, which helps prevent the two webs from deflecting laterally relative to each other. This behavior is modeled by giving the cover plate orthotropic properties, such that it has stiffness in the booster longitudinal direction, but no circumferential stiffness. The cover plate is represented with 141 plate elements, each having a thickness of .191 inches.

### Boundary Conditions

The boundary conditions at the top of the model (midway between the two webs at  $Z=0$ ) are chosen to make the X-Y or the R-theta plane a symmetry plane. This is accomplished by constraining the Z displacement and the R and theta rotations in both the case wall and cover plate nodes at  $Z=0$ . At the bottom of the model (free shell end), the theta displacement and the R and theta rotations of the case wall nodes are constrained.

### Applied Loading

The load applied to the finite element model is due to internal pressure of the SRB. The worst case value for this pressure occurring at the ET attach ring location is 912 psi and takes place during the Shuttle roll maneuver (see reference 4). The internal pressure can be resolved into a radial and an axial component as shown in figure 5. The radial

component is applied to the plate elements representing the SRB motor case wall as a uniform pressure load of 912 psi acting in the +R direction. The axial load component results from a combination of the internal pressure acting on the forward dome and the axial acceleration of the vehicle. This load tends to elongate the SRB. The dominant part of the axial force is the pressure component of 15.1 million pounds, and is obtained by integrating the internal pressure over the area of the forward dome. For the analysis presented herein, only this pressure component of axial load will be considered. The axial load is applied as a lineal load of 33078.0 pounds per inch of circumference in the -Z direction at the nodes located at the free end of the case wall.

One effect of the combined radial and axial loading which needs to be understood, is the loading induced in the ET attach ring due to the axial load component. A stiffener attached to a plate, as shown in figure 6, is given as a simplified representation of the ET attach ring attached to the SRB. When the plate is loaded in tension parallel to the stiffener, as in figure 6a, the poisson effect causes the plate to contract in a direction perpendicular to the loading, but this contraction does not add any load to the stiffener. However, when a tension load is applied perpendicular to the direction of the stiffener, as shown in figure 6b, the stiffener restrains the plate from contracting. Thus, the poisson effect now causes a compressive load to develop in the stiffener. Similarly, the axial load component in the SRB will reduce the tensile load in the ET attach ring (which is caused by the radial load component), and the importance of this effect must be assessed.

## ANALYSIS RESULTS

Both linear and nonlinear analyses were performed using the Engineering Analysis Language finite element program. The model described in the previous section was used for all analyses. In the nonlinear analysis, a full Newton-Raphson integration scheme was used to incorporate geometric nonlinearities. Additional results from a nonlinear shell analysis of the ET attach ring can be found in reference 5.

### Linear and Nonlinear Displacements

The linear and nonlinear tang deflection shapes, when both the radial and axial components of the 912 psi pressure load are applied, are shown in figures 7a and 7b respectively. The linear deflection shape for the entire model is shown in figure 7c. Load deflection curves at four locations around the tang (points A, B, C, and D of figure 3b) are shown in figure 8. For locations on the attach ring (A and C) and in the middle of

the shell (B) the linear and nonlinear displacements differ from +6.4 percent to -8.7 percent. The largest difference in radial deflections, 23.0 percent, occurs at location D.

The radial deflection at the tang is shown for the entire tang circumference in figure 9. Both linear and nonlinear deflections for the 912 psi loading (radial and axial components) are shown in the figure. The internal pressure causes the ring to open towards the ends which consequently, leads to the maximum radial deflection occurring at the ring ends. This opening of the two ends of the rings tends to straighten the 90 degree length of shell where there is no attach ring, leading to decreased radial deflections away from the ring ends (location D on figure 3b for example). Internal pressure on the section of shell between the two ring ends increases the radial deflection in this region, resulting in the bulge in radial deflection which occurs at location B. The results in figure 9 indicate that the nonlinear analysis, when compared to the linear analysis, reduces the peak radial deflections (which occur at the two ring ends), and smooths the tang radial deflections on the portion of the tang where there is no attach ring.

The tangential deflection at the tang is shown for the entire tang circumference in figure 10 (912 psi, radial and axial components). The figure indicates that uniform radial expansion is occurring in the center portion of the tang away from the web ends (since the tangential displacement is approximately zero). Including geometric nonlinearities in the analysis reduces the peak tangential displacements at the ends of the webs by approximately 50 percent from those predicted by the linear analysis.

Radial deflections along the SRB motor case wall (from the symmetry plane to the bottom of the model) are shown for three locations (corresponding to points A, B, and C in figure 3b) in figure 11. Linear and nonlinear results are shown for 912 psi internal pressure with both radial and axial loading components. The corresponding radial displacement for a cylinder with spherical end caps, SRB properties, and subjected to an internal pressure of 912 psi, is .230 inches when the wall thickness is .58 inches, and .279 inches when the wall thickness is .479 inches (see reference 3). Compared to the linear analysis, the nonlinear results predict a maximum radial deflection along the motor case which is 5.1 percent less at the circumferential location corresponding to point A, 8.8 percent less at location B, and 12.6 percent less at location C. At the bottom of the model however, all nodes around the circumference of the model have radial displacements which are within 4.5 percent of the theoretical radial displacement of .279 inches.

## Linear and Nonlinear Stresses

Table 1 shows the circumferential stresses in the ET attach ring model due to an internal pressure of 912 psi for two cases; 1) radial loading component only, and 2) both axial and radial loading components. The stresses shown are taken at the section labeled A-A on figure 3b (the portion of the ring midway between the two ring ends). The compressive stress induced by the poisson effect (as discussed in figure 6) reduces the stress levels in all of the ET attach ring components by approximately 18 percent. The maximum circumferential stress in the web, 121.2 ksi, occurs near the end of the web and is approximately twice the average value of stress found at section A-A.

Circumferential stresses in the ET attach ring model are shown along the length of the case wall at section B-B (see figure 3b) in Table 2. The boundaries and thicknesses of the plate elements making up the shell are indicated, with the ET attach ring being attached at the boundary between the second and third element from the top. Stresses due to 912 psi internal pressure are given for two cases; 1) radial loading component only, and 2) both axial and radial loading components. The finite element stresses are compared to stresses calculated from a simple closed form solution for a thin shell (stress = pressure x radius / thickness). As expected, the axial load component has negligible effect on the circumferential stresses in the case wall. In the vicinity of the ring, the case wall circumferential stresses are approximately 10 percent less than those predicted by the simple closed form solution. Away from the attach ring however, the finite element and analytical solutions agree to within 1 percent.

The bending moment resultant,  $M_{\theta}$ , along the length of the case wall is shown at three circumferential locations (corresponding to points A, B, and C in figure 3b) in figure 12. In general, the bending moment at all three locations have peaks where the ET attach ring is attached to the case, and where the case wall thickness decreases from .58 inches to .479 inches (the two places where stiffness changes in the case wall occur). For the two locations which include the web (A and C), the peaks due to the attach ring are much greater than those due to the thickness change in the case wall. The ET attach ring also affects the area of shell away from the two ring ends (location B) as indicated by the small peak in curve B where the ET attach ring is connected to the case wall. Since the moment at all three locations approaches zero at the bottom of the shell, an adequate length of case wall has been included in the model.

The shear stress resultant,  $N_{R\theta}$ , at the web/tang interface is shown in figure 13. The large spikes in shear stress near the web ends indicate



that the web is attempting to peel away from the case wall in these locations. These spikes in shear stress also occur at the same locations where failed and yielded bolts occurred in the flight and ground test hardware (see reference 1).

Stresses due to the 912 psi internal pressure load (radial and axial components) and calculated from the linear and nonlinear analyses are compared for the various components of the ET attach ring model in Table 3. This table only includes the circumferential membrane resultant stress at the center of the plate elements, and only the axial stress for the beam elements. The table indicates that nonlinearities have a moderate (less than 8 percent) effect on average element stresses.

However, nonlinearities can have a larger effect on element stress components when bending is included. Table 4 shows the maximum total stress in the tang at one of the web ends. The nonlinear solution gives a 3.8 percent reduction in the tang axial load (consistent with the results shown in the previous table) and a 13.5 percent reduction in the tang bending moment. Thus, the maximum stress in the tang outer fiber is reduced by 7.5 percent in the nonlinear solution.

#### Effect of SRB Field Joint on ET Attach Ring

In the actual SRB motor case, the center of the aft attachment segment field joint is located 19.5 inches above the midpoint between the two webs of the ET attach ring. A simplified representation of the field joint (see reference 5) is added to the attach ring model to determine the effect of the field joint on attach ring stresses. The field joint is represented by an annulus with a width of 6 inches and a thickness of 1.1 inches, and is centered 13.5 inches from the center of the tang. Because of the symmetry boundary condition imposed at the top of the model however, a structure with a field joint on both sides of the ET attach ring is actually being modeled.

The variation in radial deflection along the length of the case wall at two circumferential locations (A and B on figure 3b) is shown in figure 14. Results derived with and without the field joint in the model, and due to the 912 psi pressure load (radial plus axial components) are compared. Adding the field joint greatly reduces the case wall radial deflections in the vicinity of the joint, and slightly increases the radial deflections at the bottom of the model away from the joint. In Table 5, the circumferential stresses at section A-A (see figure 3b) of the ET attach ring are shown with and without the field joint in the model. Including the field joint in the model has very little effect (less than 2 percent) on stresses in the ET attach ring.

## CONCLUSIONS

External Tank (ET) attach rings are used to transfer lateral loads between the Space Shuttle ET and the two Solid Rocket Boosters (SRBs). Following the Challenger (51-L) accident, review of the flight performance history of the ET attach ring revealed the repeated occurrence of failed bolts in the ring. Subsequent analysis showed that negative margins of safety occur in the existing ring during the shuttle roll maneuver when the internal pressure in the SRB rises to its maximum value of 912 psi at the attach ring station. The linear and nonlinear finite element analyses described in this report were performed to aid in a ET attach ring redesign effort undertaken by NASA Langley Research Center, as well as to understand the ET attach ring structural response to motor case internal pressurization.

The axial load component reduces the stresses in the ET attach ring because of the poisson effect, with the amount of stress reduction increasing with increasing axial load. This result is especially significant because inertia effects and gas flow through the rocket nozzle reduce the axial load in the SRB from the value that is calculated by integrating the pressure over the forward dome. Thus, using the integrated pressure leads to the calculation of nonconservative stresses in the ET attach ring.

The nonlinear analysis generally gave higher stresses (maximum of 7 percent) in the cap, in the low stressed portions of the tang, and in the web. However, the nonlinear analysis gave lower stresses in the highly stressed portions of the tang. Thus, margins of safety which are less than 8 percent and are derived from linear analysis should be checked against component location to insure a conservative 270-degree ET attach ring design.

Finally, analyses indicated that including the field joint in the model does not change stresses in the ET attach ring significantly. This result is important because none of the detailed analyses being performed for the redesign effort include the field joint or its effects in their models and this result validates that assumption.

## REFERENCES

1. McComb, Harvey G. Jr. (Compiler); et al: Redesign of Solid Rocket Booster/External Tank Attachment Ring for the Space Transportation System. NASA TM-100476, July 1987.
2. Whetstone, W. D.: Engineering Analysis Language Reference Manual. Engineering Information Systems, Inc., San Jose, California. August 1985.
3. Timoshenko, S.; and Woinowsky-Krieger, S.: Theory of Plates and Shells, 2nd. Edition. McGraw-Hill Book Company, New York, 1959.
4. Interim IVBC-3 Design Loads for use in SRB and SRM Steel Case Redesign and Recertification, Marshall Space Flight Center letter from ED01/Dr. McDonough to SA41/Mr. Smith, December 16, 1986.
5. Knight, Norman F. Jr.: Nonlinear Shell Analyses of the SRB/ETA Ring Interface. NASA TM-89164, July 1987.

TABLE 1.-EFFECT OF AXIAL LOAD COMPONENT ON ET ATTACH RING STRESSES.  
(912 psi internal pressure)

STRESS, ksi	
Radial plus axial load components	Radial load component only
45.1	54.6
49.3	60.2
50.8	62.0
52.4	64.1
53.5	66.0
57.2	69.8
78.4	74.5

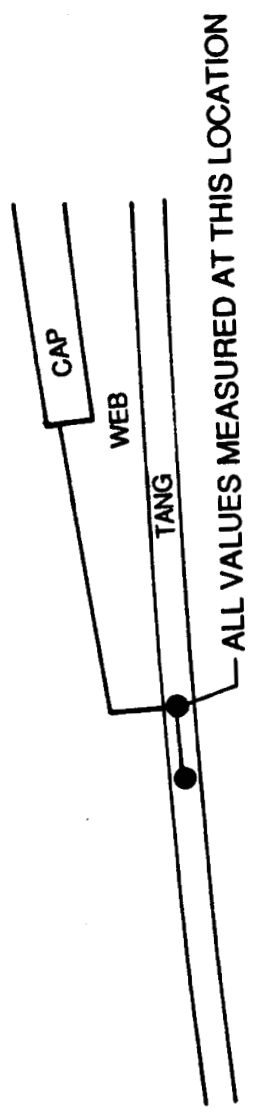
TABLE 2.-EFFECT OF AXIAL LOAD COMPONENT ON MOTOR CASE STRESSES.  
(912 psi internal pressure)

Analytical solution	STRESS, ksi	
	Radial plus axial component	Radial component only
114.5	101.7	101.8
114.5	101.1	102.0
114.5	103.6	105.5
114.5	111.3	113.0
125.4	122.7	120.9
138.6	135.7	130.4
138.6	140.9	138.2
138.6	139.0	139.4

TABLE 3.-COMPARISON OF LINEAR AND NONLINEAR STRESSES.  
(912 psi internal pressure)

Component+	STRESS, ksi		$\Delta$ %
	Linear	Nonlinear	
CAP (Max)	46.5	49.0	+5.4
TANG (Section A-A)	57.2	60.9	+6.5
Web end (Max)	139.3	130.3	-6.4
CASE WALL			
WEB (Section A-A)	50.8	54.2	+6.6
End (Max)	121.2	128.0	+5.6

TABLE 4.-LOCAL TANG BENDING AT END OF WEB.  
(912 psi internal pressure)



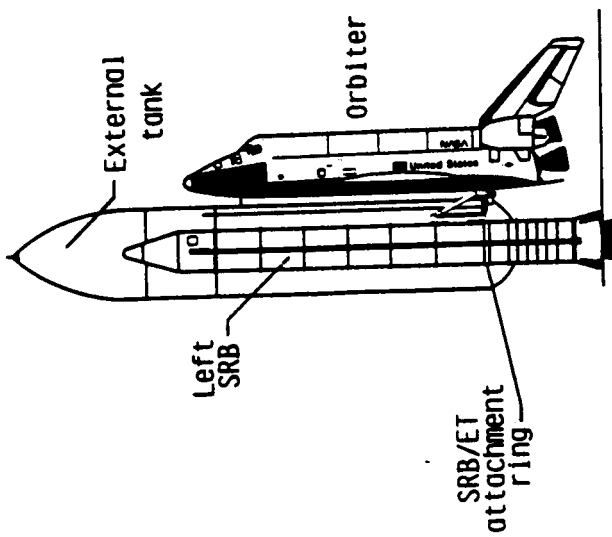
	LINEAR	NONLINEAR	Δ %
PZ, lbf	88505.	85156.	-3.78
MY, in-lbf	15457.	13378.	-13.45
σ* <sub>MAX</sub> , ksi	218.5	202.1	-7.53

$$\sigma^* = \frac{PZ}{A} + \frac{MY \times Z}{I} : A = .6616 \text{ in}^2 \quad Z = .827 \text{ in} \quad I = .1508 \text{ in}^4$$

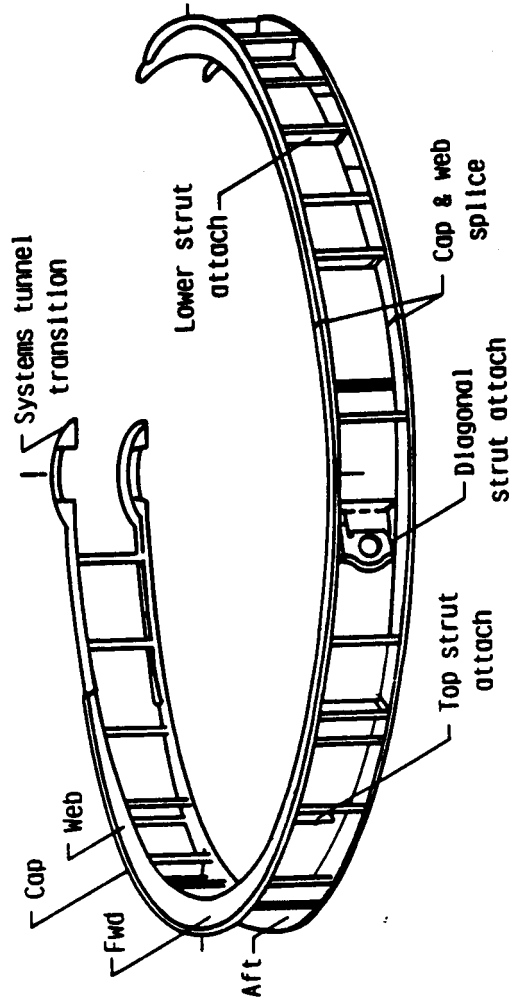
TABLE 5.-EFFECT OF FIELD JOINT ON RING STRESSES.  
(912 psi internal pressure)

STRESS, ksi		Δ %
No field joint	With field joint	
45.1	45.8	+1.6
49.3	49.7	+0.8
50.8	51.2	+0.8
52.4	52.8	+0.8
53.5	54.4	+1.7
57.2	57.5	+0.5
78.4	78.2	-0.3



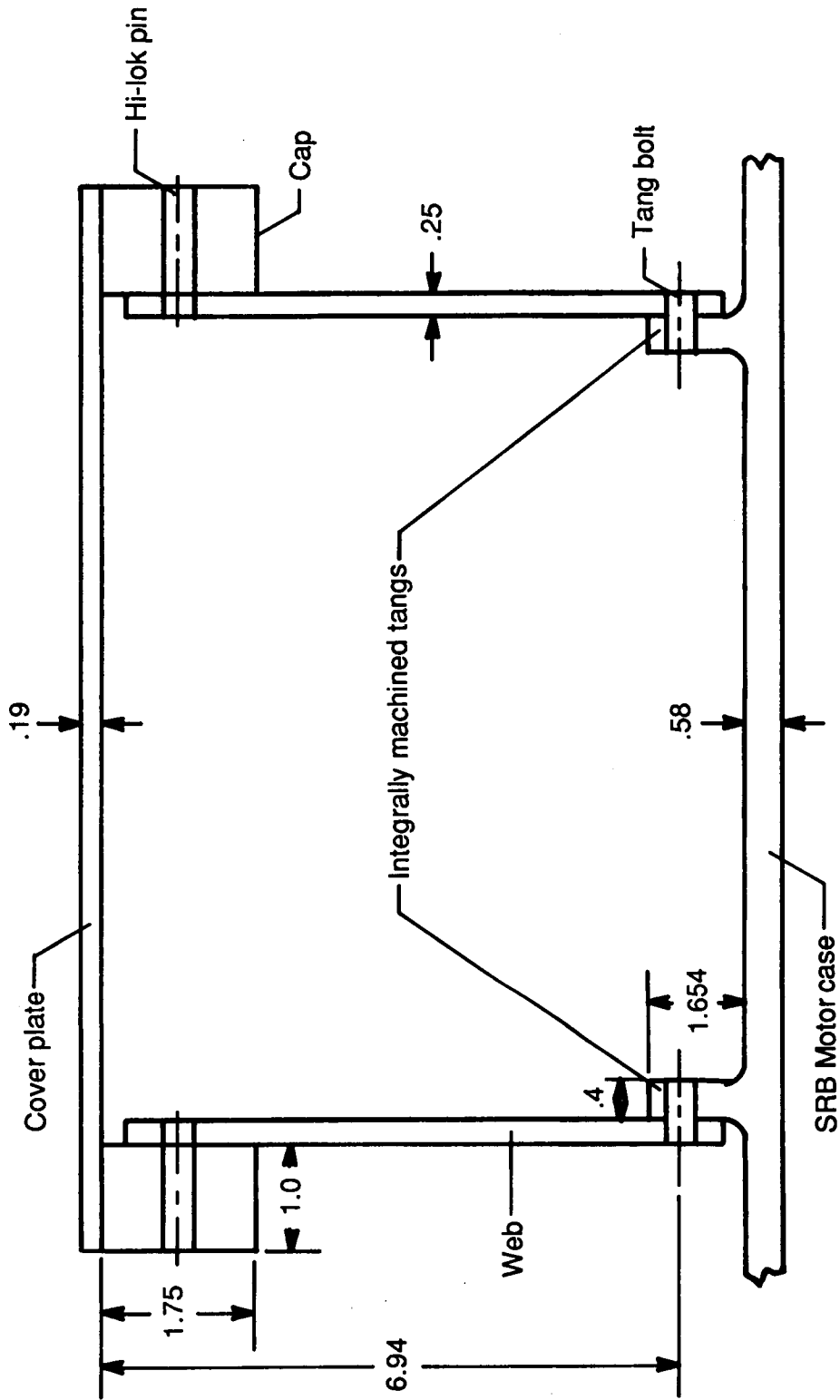


a. Left side view of Space Shuttle system.



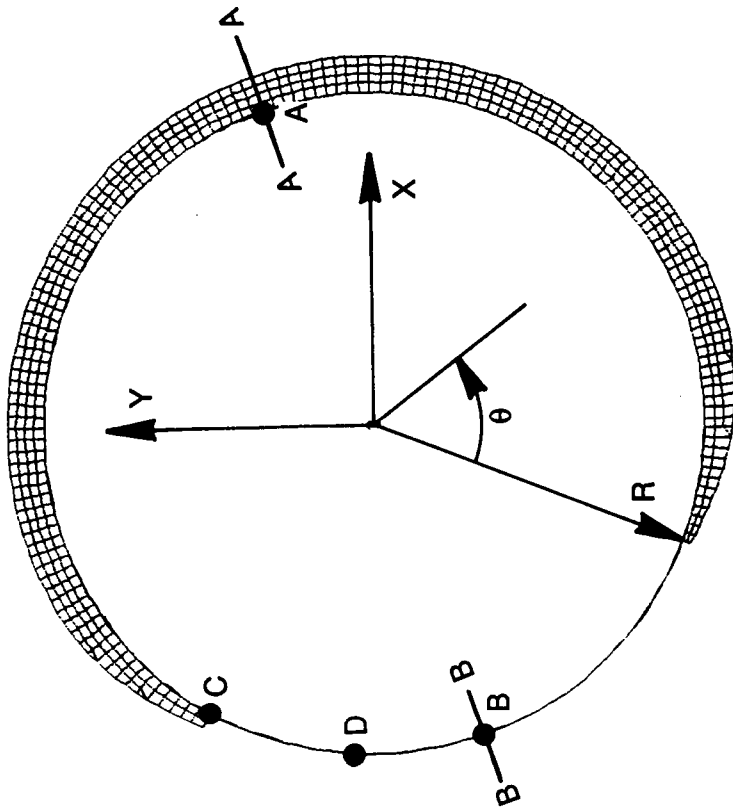
b. Left SRB/ET attach ring-existing design.

Figure 1. Overview of SRB/ET attach ring subsystem.

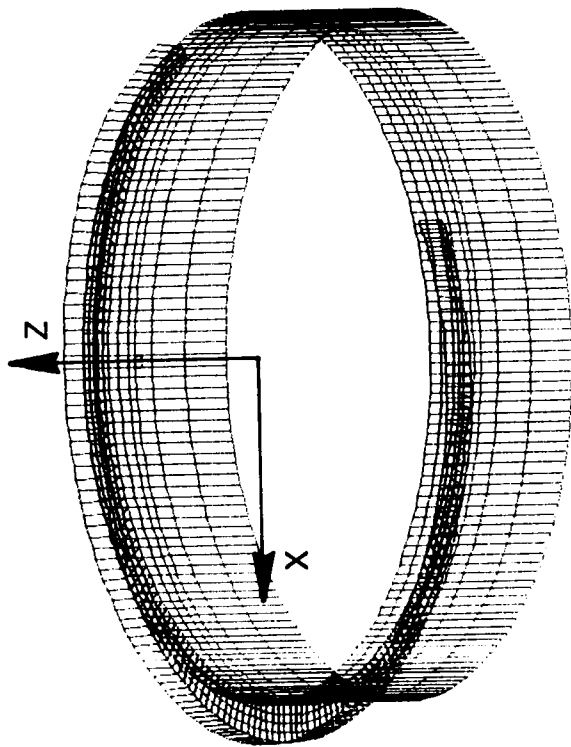


Note: All dimensions are in inches.

Figure 2. External tank attach ring cross section.



b. Web platform.



a. Full model.

Figure 3. SRB/ET attach ring finite element analysis model.

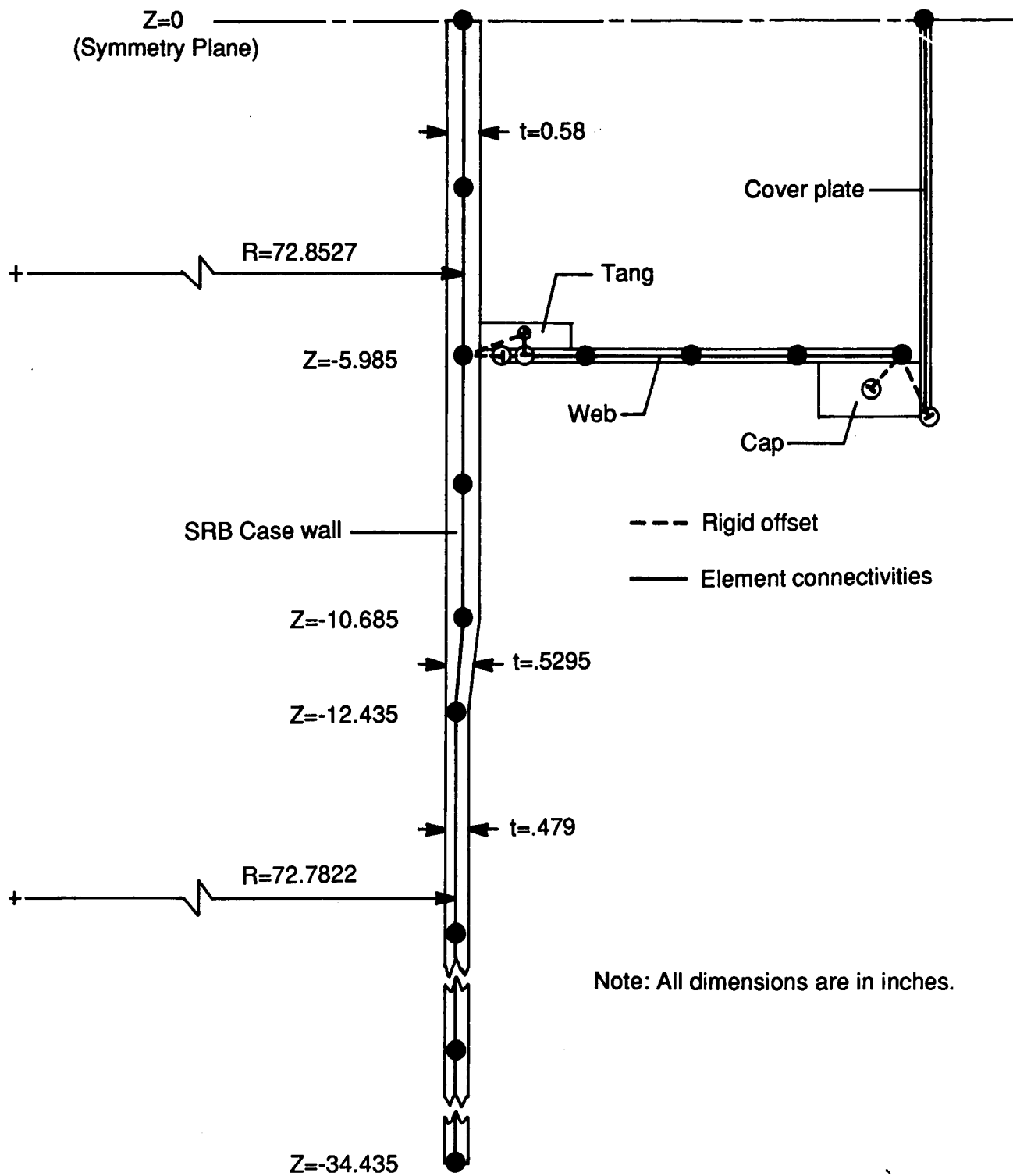


Figure 4. Cross section of finite element model.

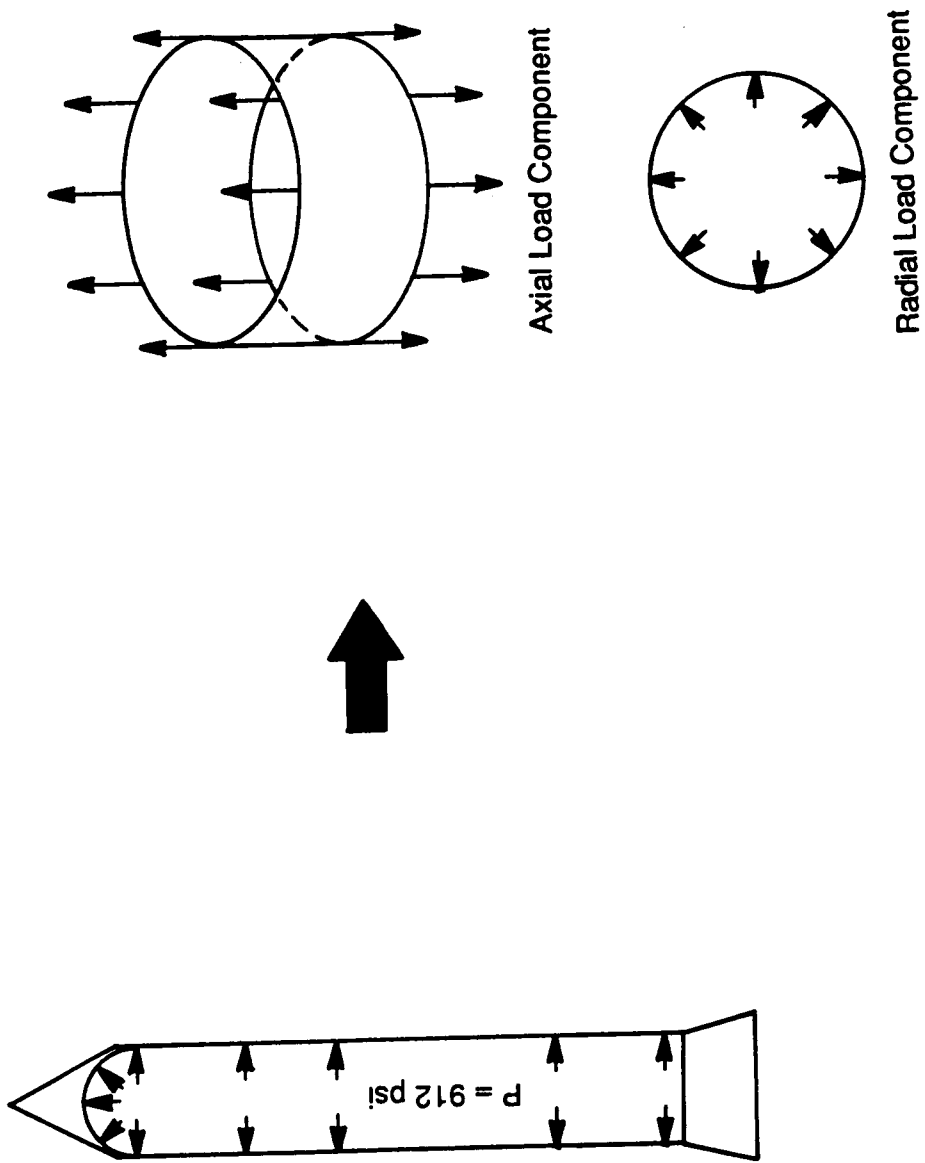
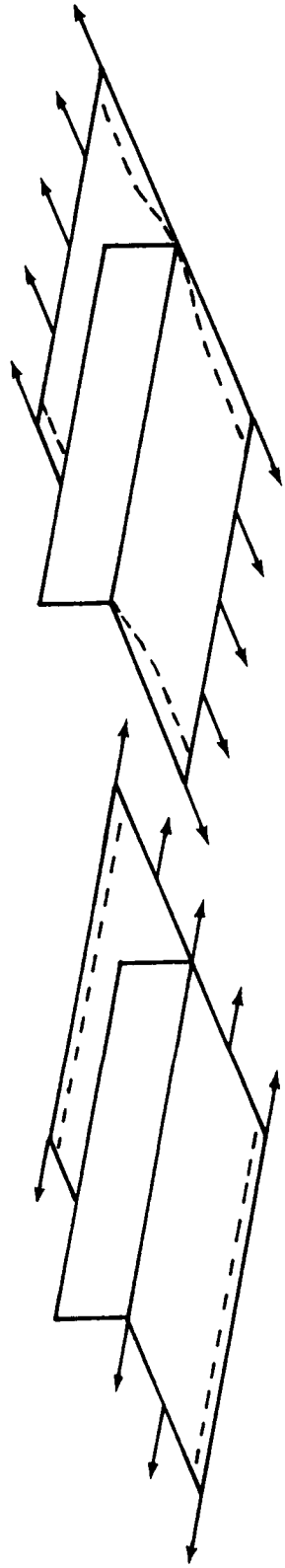


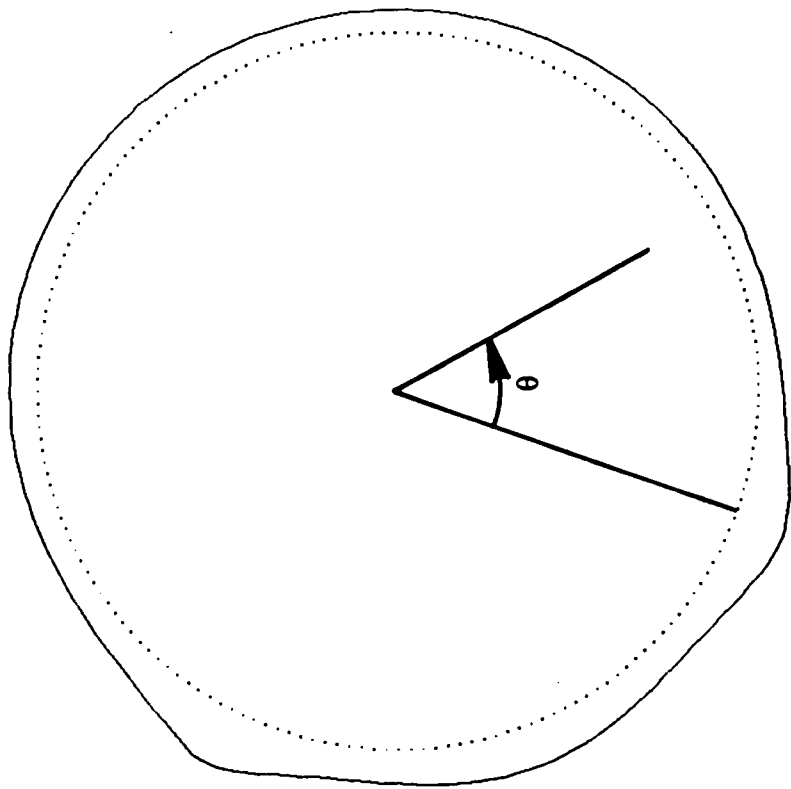
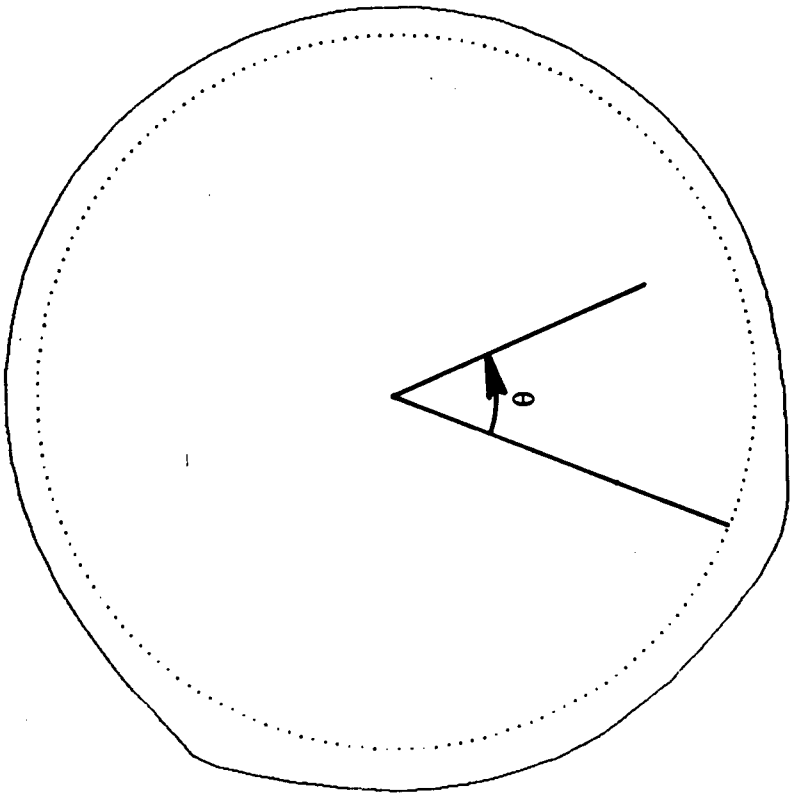
Figure 5. Applied loads for ET attach ring finite element model.



a. Poisson effect causes no load in the stiffener.

b. Poisson effect causes compression load in the stiffener.

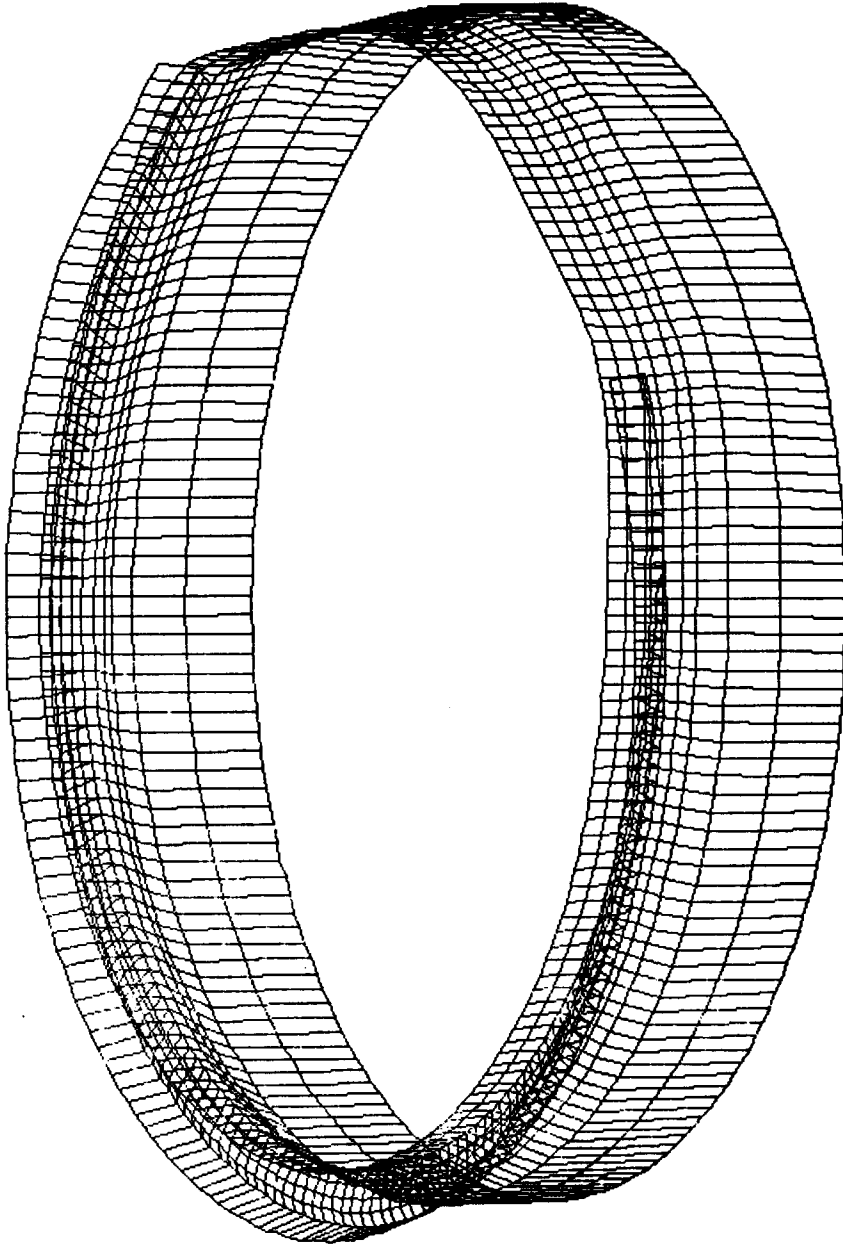
Figure 6. SRB applied axial load affects attach ring stresses.



a. Tang-linear deflection.

b. Tang-nonlinear deflection.

Figure 7. ET attach ring deflections due to 912 psi internal booster pressure (radial plus axial components).



c. Full model-linear deflection.

Figure 7. Concluded.



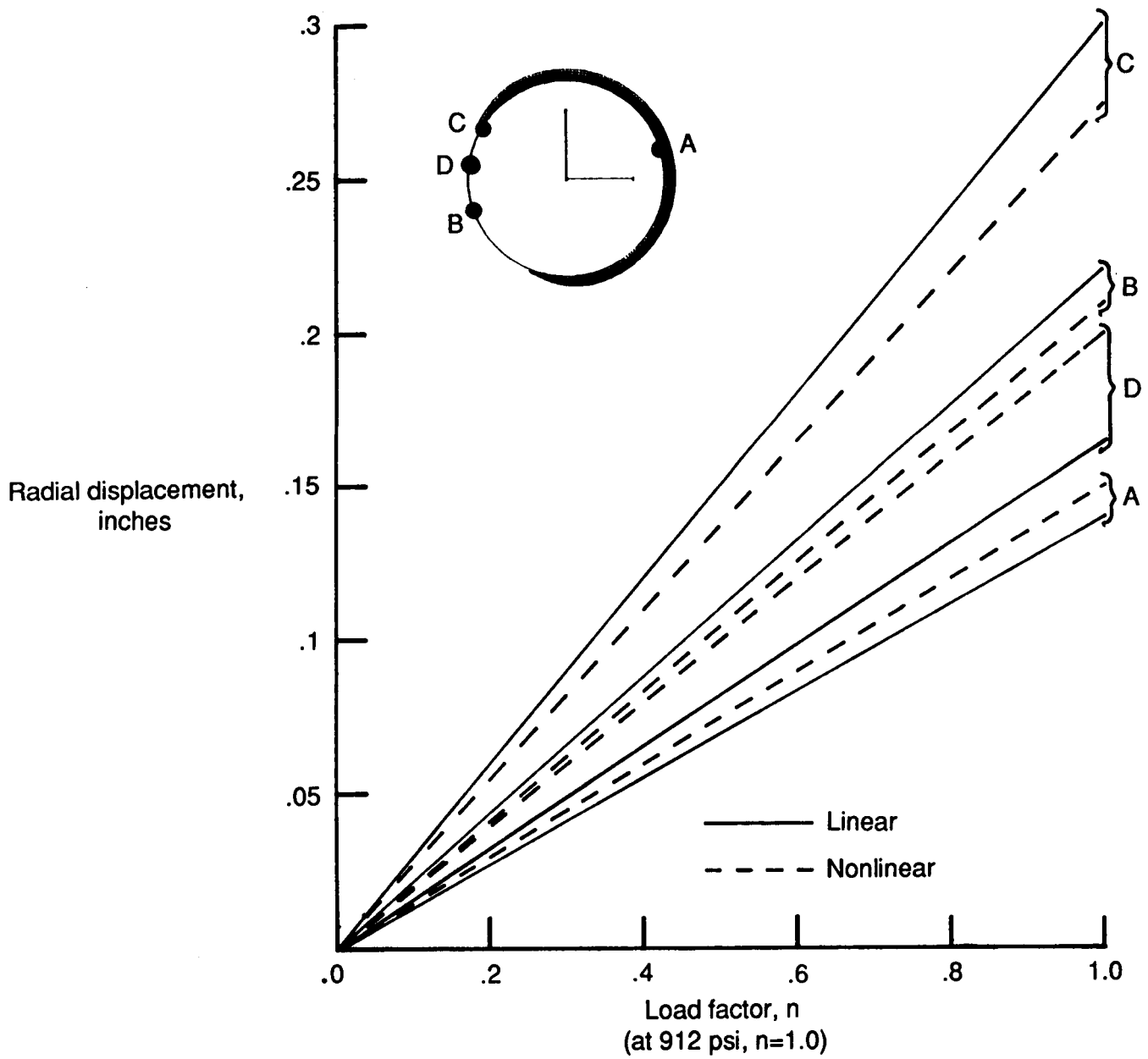


Figure 8. Variation of radial displacement with load (912 psi internal pressure) at four tang locations.

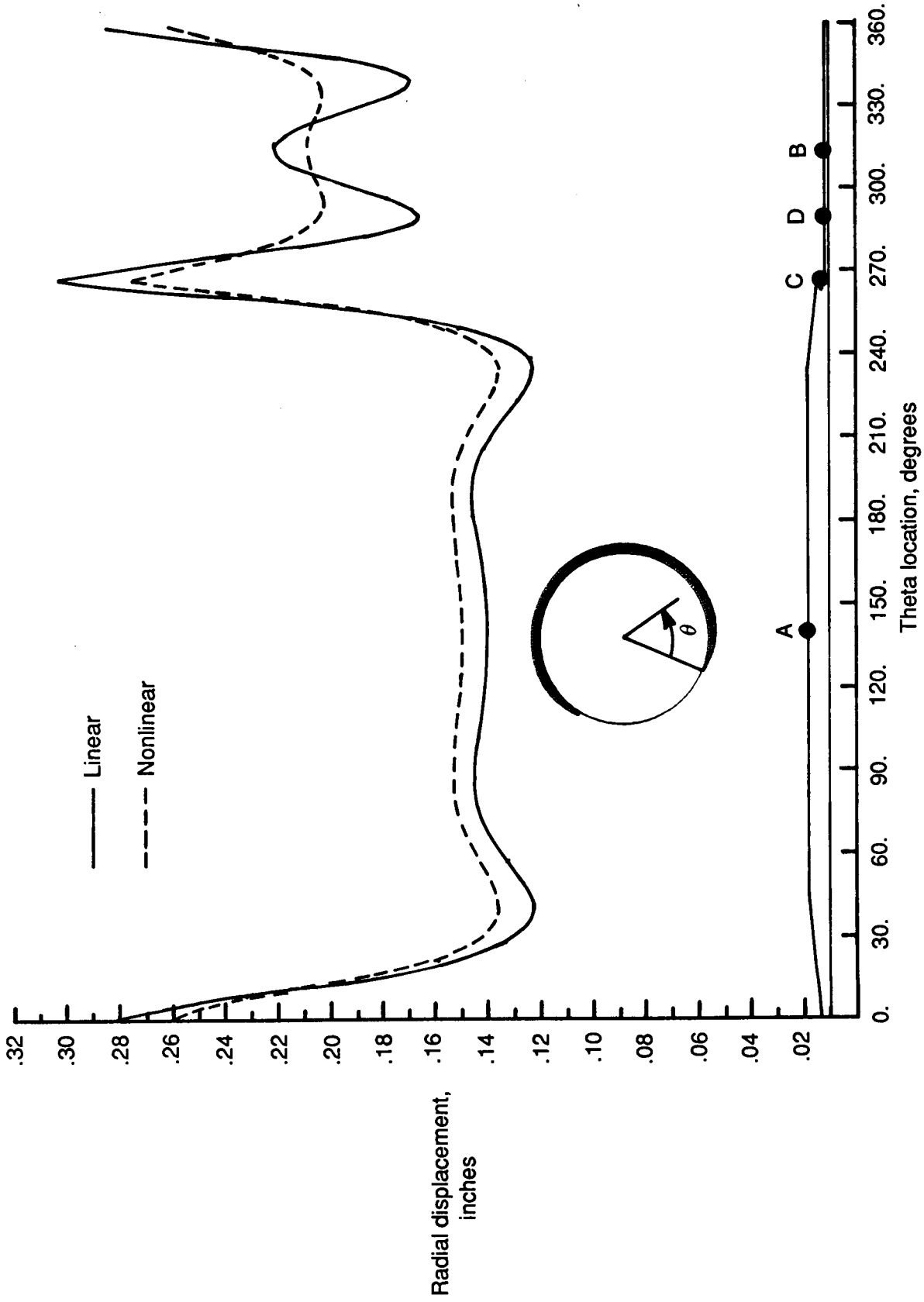


Figure 9. Tang radial displacement due to 912 psi internal pressure.

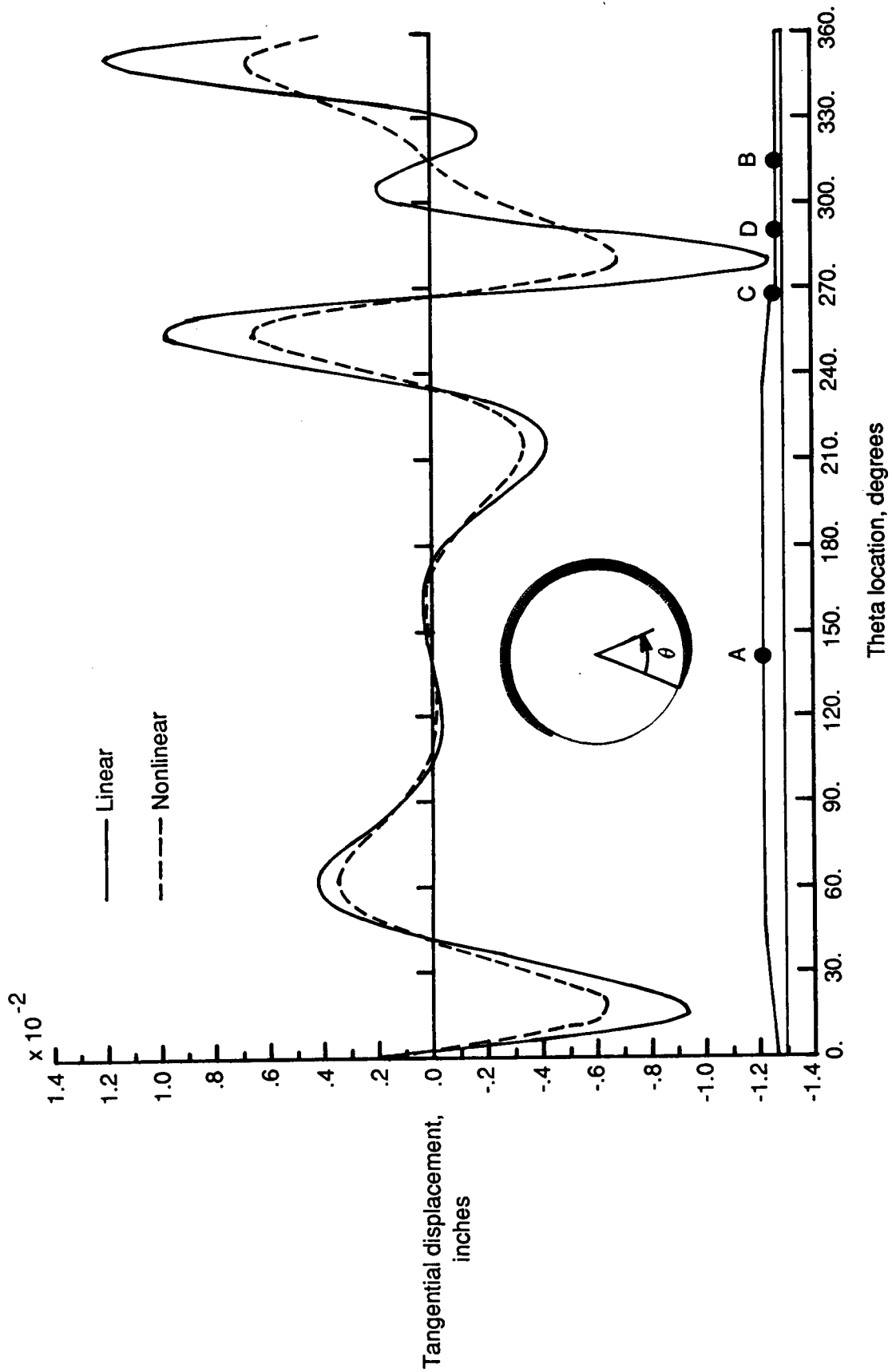


Figure 10. Tangential displacement due to 912 psi internal pressure.

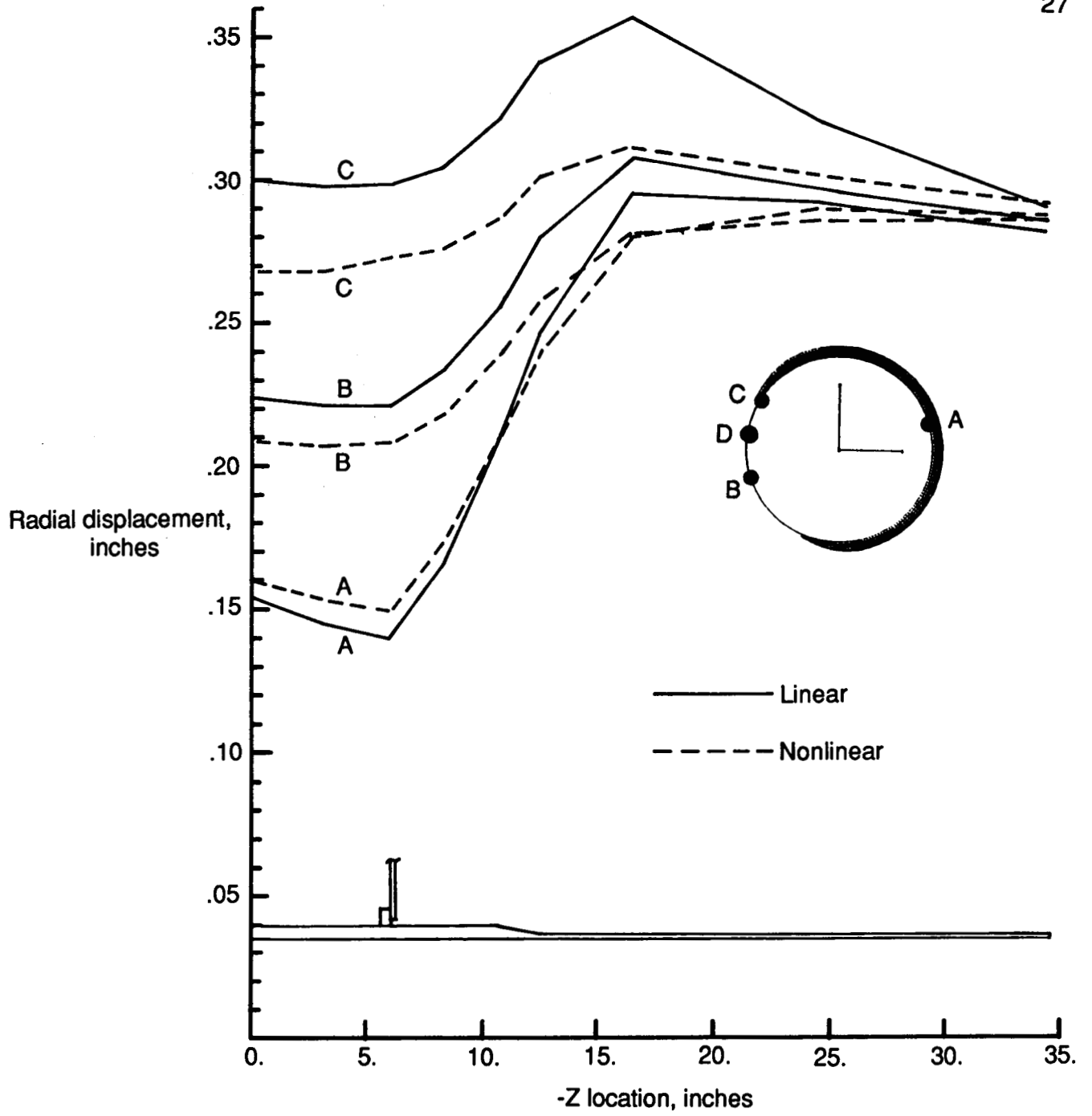


Figure 11. Radial displacement along rocket motor case due to 912 psi internal pressure.

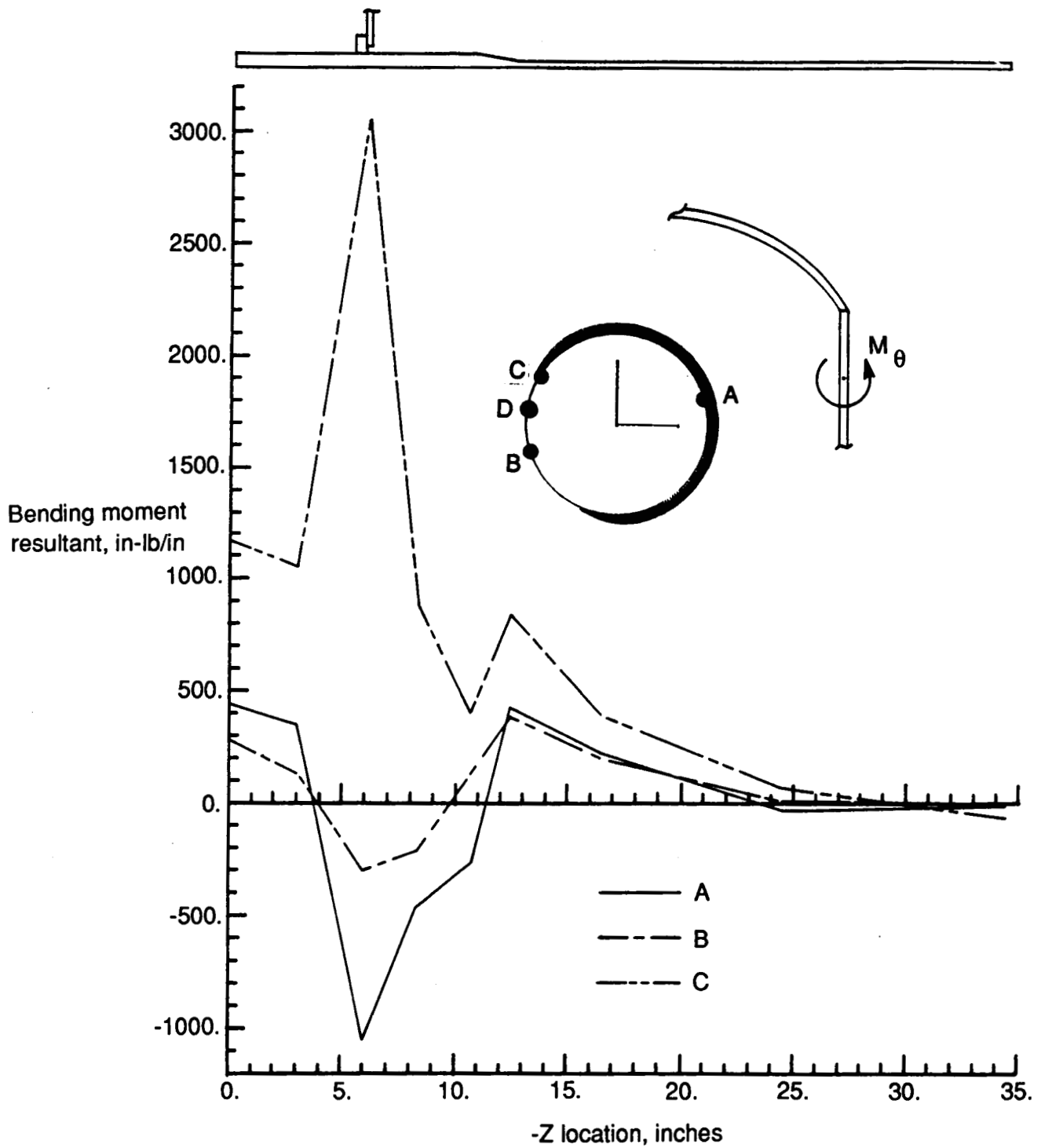


Figure 12. Bending moment resultant along case wall due to 912 psi internal pressure loading.

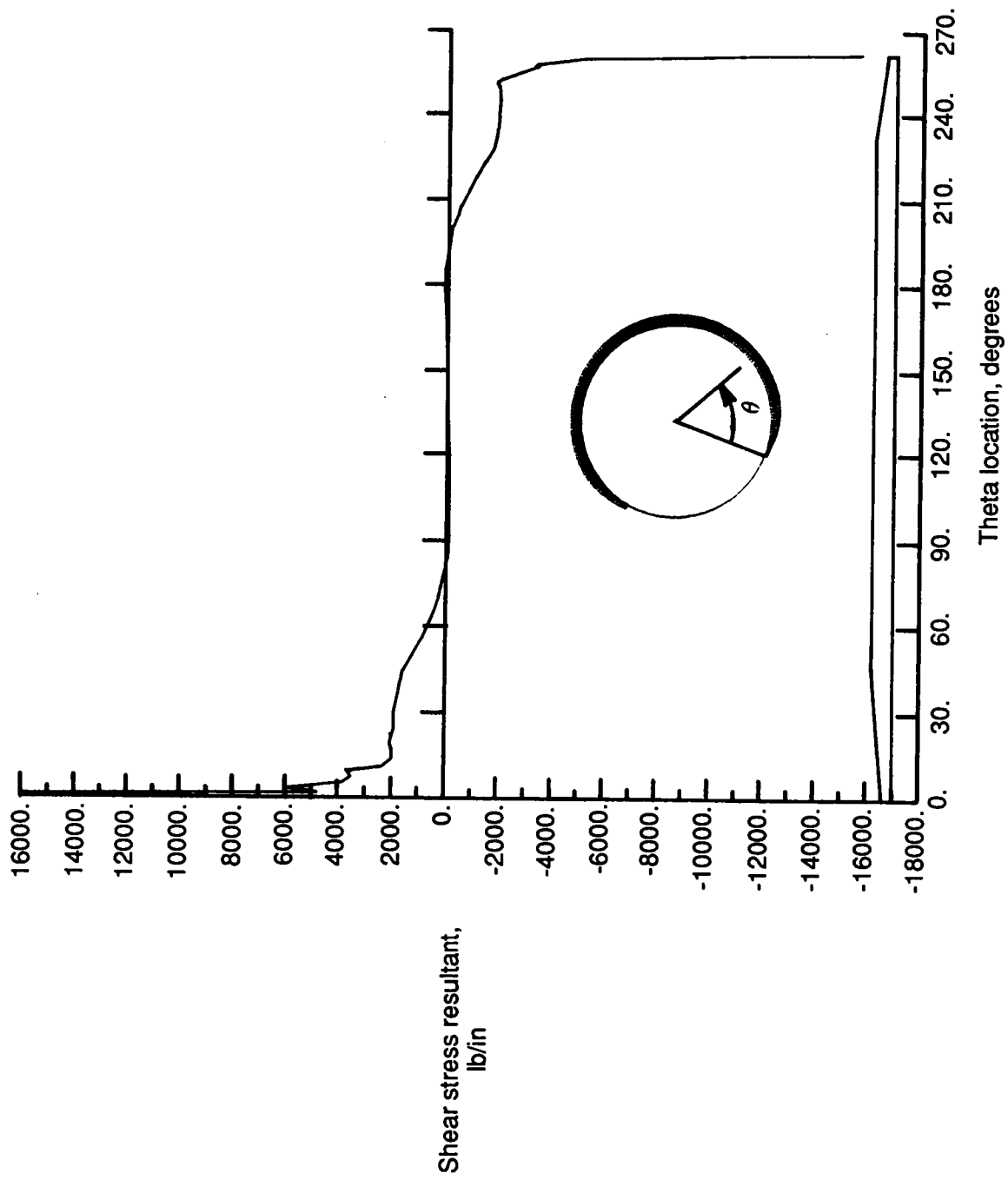


Figure 13. Linear shear stress distribution at tang/web interface (912 psi internal pressure loading).

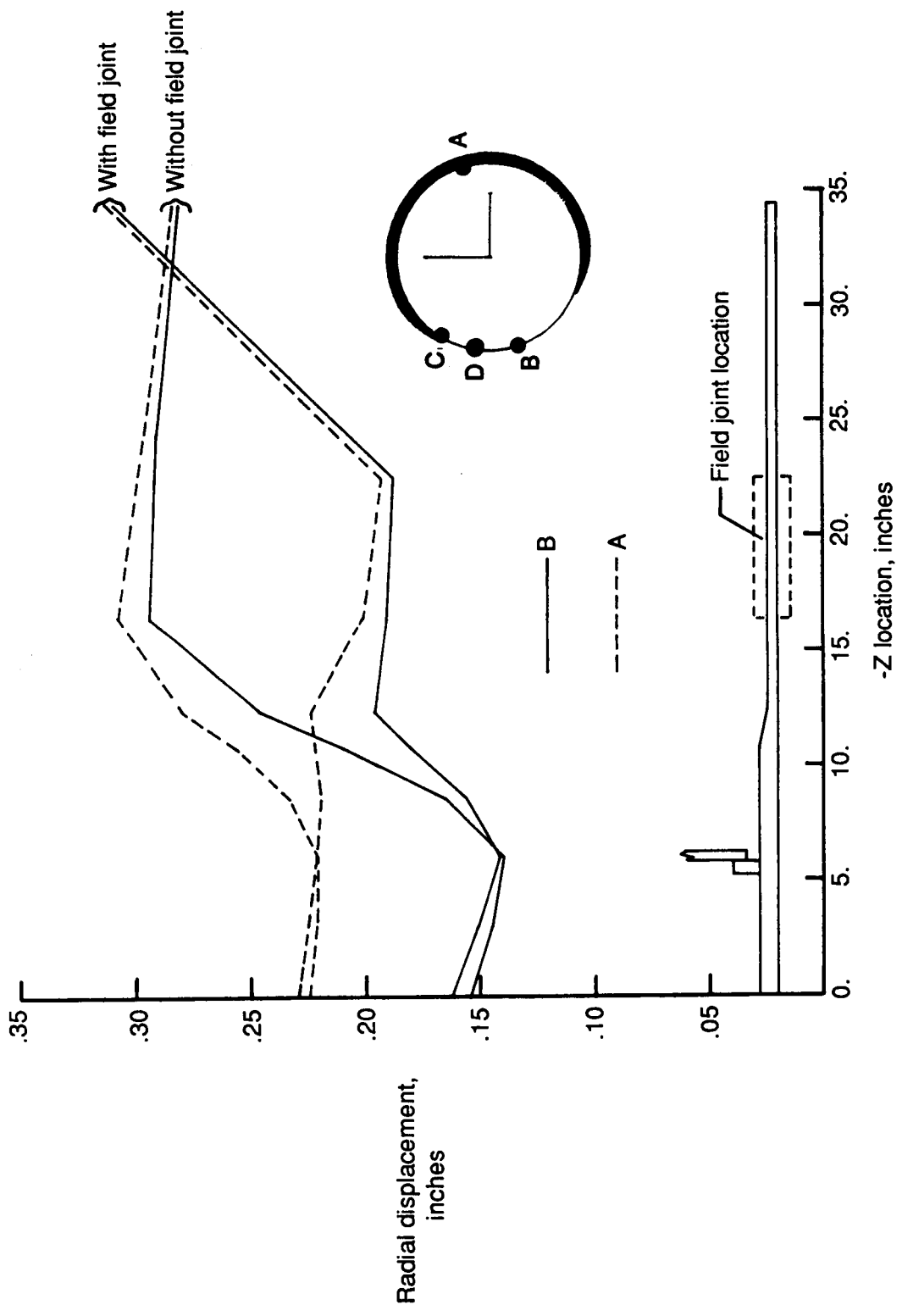


Figure 14. Effect of field joint on motor case displacements.



# Report Documentation Page

1. Report No. <b>NASA TM-100510</b>		2. Government Accession No.		3. Recipient's Catalog No.	
4. Title and Subtitle <b>Structural Analysis of the Space Shuttle Solid Rocket Booster/External Tank Attach Ring</b>				5. Report Date <b>January 1988</b>	
				6. Performing Organization Code	
7. Author(s) <b>John T. Dorsey</b>				8. Performing Organization Report No.	
				10. Work Unit No. <b>506-43-41-02</b>	
9. Performing Organization Name and Address <b>NASA Langley Research Center Hampton, VA 23665-2552</b>				11. Contract or Grant No.	
				13. Type of Report and Period Covered <b>Technical Memorandum</b>	
12. Sponsoring Agency Name and Address <b>National Aeronautics and Space Administration Washington, DC 20546</b>				14. Sponsoring Agency Code	
				15. Supplementary Notes	
16. Abstract <p>An External Tank (ET) attach ring is used in the Space Shuttle System to transfer lateral loads between the ET and the Solid Rocket Booster (SRB). Following the Challenger (51-L) accident, the flight performance of the ET attach ring was reviewed, and negative margins of safety and failed bolts in the attach ring were subsequently identified. The analyses described in this report were performed in order to understand the existing ET attach ring structural response to motor case internal pressurization as well as to aid in an ET attach ring redesign effort undertaken by NASA LaRC. The finite element model as well as the results from linear and nonlinear static structural analyses are described.</p>					
17. Key Words (Suggested by Author(s)) <b>Space Shuttle Solid Rocket Booster External Tank Attach Ring Structural Analysis</b>			18. Distribution Statement <b>Unclassified - Unlimited  Subject Category - 18</b>		
19. Security Classif. (of this report) <b>Unclassified</b>		20. Security Classif. (of this page) <b>Unclassified</b>		21. No. of pages <b>31</b>	22. Price <b>A03</b>